Atomic processes in bicircular fields

Atomic processes in bicircular fields

S Odžak[1], E Hasović[1], W. Becker[2] and D B Milošević[1,2,3]

[1] Faculty of Science, University of Sarajevo, Zmaja od Bosne 35, 71000 Sarajevo, Bosnia and Herzegovina
[2] Max-Born-Institut, Max-Born-Str. 2a, 12489 Berlin, Germany
[3] Academy of Sciences and Arts of Bosnia and Herzegovina, Bistrik 7, 71000 Sarajevo, Bosnia and Herzegovina

E-mail:
senad.odzak@gmail.com,ahasovic1@yahoo.com,wbecker@mbi-berlin.de,milo@bih.net.ba

Abstract. We investigate laser-assisted electron-ion recombination (LAR), high-order harmonic generation (HHG) and above-threshold ionization (ATI) of argon atoms by a bicircular laser field, which consists of two coplanar counter-rotating circularly polarized fields of frequencies $r\omega$ and $s\omega$. The energy of soft x rays generated in the LAR process is analyzed as a function of the incident electron angle and numerical results of direct recombination of electrons with Ar^+ ions are presented. We also present the results of HHG by a bicircular field and confirm the selection rules derived earlier for inert-gas atoms in a p ground state. We show that the photoelectron spectra in the ATI process, presented in the momentum plane, as well as the LAR spectra exhibit the same discrete rotational symmetry as the applied field.

1. Introduction

Various nonlinear processes can occur when atoms or molecules are exposed to intense laser fields [1, 2]. Generally, these processes can be categorized into two groups: laser-assisted processes and laser-induced processes. The first group includes phenomena that can occur without the presence of a laser field, such as laser-assisted electron-atom scattering and laser-assisted electron-ion recombination (LAR) [3]. In contrast, laser-induced processes cannot happen except in the presence of a laser field. Examples of such processes are high-order harmonic generation (HHG) and above-threshold ionization (ATI) [4]. In the last two decades, all of these processes have been investigated in detail by considering atoms or molecules interacting with linearly polarized laser fields.

It was almost generally accepted that HHG and high-order above-threshold ionization (HATI) will be inefficient unless the laser polarization is linear. Otherwise, an electron that starts its orbit with zero velocity will almost never revisit its parent ion. For linear polarization, the electron trajectories are one-dimensional and along the direction of the linearly polarized driving laser field. However, already 20 years ago a scheme for efficient HHG in two dimensions was realized [5, 6], and 15 years ago its properties were investigated in detail and explained [7, 8, 9, 10, 11, 12]. This scheme employed a bicircular field, which consists of two coplanar counterrotating circularly polarized fields with frequencies that are integer multiples of a fundamental laser frequency. Very recently, this scheme has attracted great attention [13, 14, 15, 16, 17, 18, 19, 20, 21]. This is because a bicircular field generates harmonics that are circularly polarized (in addition to being bright). Related schemes employ a circularly polarized

field plus a static magnetic field [22, 23] or crossed-beam two-color fields [24]. Bright circularly polarized harmonics open up possibilities for various applications, for example, for photoelectron circular dichroism in chiral molecules or x-ray magnetic circular dichroism spectroscopy, two important areas of chemistry and solid state physics.

In the present contribution we consider various atomic processes driven by a bicircular field. From the first-order processes we consider (direct) ATI and LAR and present a symmetry analysis of the angle-resolved ATI electron spectra and the emitted x-ray spectra. We will also consider higher-order processes such as HHG and HATI. Our underlying theory, which is based on the S-matrix formalism, is presented in Sec. 2 while the bicircular field and the corresponding symmetry analysis are presented in Sec. 3. Our numerical results are presented and discussed in Sec. 4 and finally our conclusions are summarized in Sec. 5. The atomic system of units ($\hbar = e = m_e = 4\pi\varepsilon_0 = 1$) is used throughout the paper.

2. Theory

In the present paper we use an S-matrix approach to describe the above-mentioned processes occurring in the presence of intense laser fields. In order to model the interaction of the strong laser field with atoms we use the single-active-electron approximation and the dipole approximation. The corresponding Hamiltonian can be written as

$$H(t) = -\frac{\boldsymbol{\nabla}^2}{2} + \mathbf{r}\cdot\mathbf{E}(t) + V(\mathbf{r}), \tag{1}$$

where $\mathbf{r}\cdot\mathbf{E}(t)$ is the laser field-electron interaction in the length gauge and $V(\mathbf{r})$ is the interaction of the electron with the rest of the atom in the absence of the laser field. The S-matrix element for a transition from an initial state $|\psi_i\rangle$ to a final state $|\psi_f\rangle$ is given by

$$S_{fi} = i \lim_{\substack{t\to\infty \\ t'\to-\infty}} \langle\psi_f(t)|U(t,t')|\psi_i(t')\rangle, \tag{2}$$

where $U(t,t')$ is the time evolution operator, which is a solution of the Schrödinger equation with the Hamiltonian (1). For the LAR (HHG, HATI) process the initial state is the unbound laser-free state $|\psi_i\rangle = |\mathbf{p}\rangle$ (atomic laser-free ground state $|\psi_B\rangle$) with $\langle\mathbf{r}|\mathbf{p}\rangle = (2\pi)^{-3/2}\exp(i\mathbf{p}\cdot\mathbf{r})$. The final state of the HATI (LAR, HHG) process is the continuum state $|\mathbf{p}\rangle$ (atomic bound state $|\psi_B\rangle$). In order to calculate the transition amplitude from the initial to the final state we use the strong-field approximation (SFA) in all of the above-mentioned processes [4, 1].

In the case of the direct LAR process the incident electron with momentum $\mathbf{p}$ recombines with the positive ion and an atomic bound state with energy $E_B < 0$ is formed. This process happens in the presence of a strong periodic laser field, which is defined by the electric field vector $\mathbf{E}(t)$, with the period T and frequency $\omega = 2\pi/T$, followed by emission of an x-ray photon with wave vector $\mathbf{K}$, frequency $\omega_{\mathbf{K}}$ and unit complex polarization vector $\hat{\mathbf{e}}_{\mathbf{K}}$. The LAR process is characterized by the differential power spectrum [3]

$$S(\mathbf{K},\mathbf{p}) = \frac{p\omega_{\mathbf{K}}^4}{2\pi c^3}\left|T_n\right|^2, \tag{3}$$

where $T_n = \mathbf{T}(\mathbf{K},\mathbf{p})\cdot\hat{\mathbf{e}}^*_{\mathbf{K}}$ is the T-matrix element. The number of photons n exchanged with the laser field is obtained from the energy-conserving condition

$$n = (\omega_{\mathbf{K}} + E_B - E_{\mathbf{p}} - U_{\mathrm{P}})/\omega, \tag{4}$$

where $E_{\mathbf{p}} = \mathbf{p}^2/2$ is the energy of the incident electron, $U_{\mathrm{P}} = \int_0^T \mathbf{A}^2(t)dt/(2T)$ is the ponderomotive energy and $\mathbf{A}(t) = -\int^t \mathbf{E}(t')dt'$ the vector potential. In length gauge and

dipole approximation we have

$$\mathbf{T}(\mathbf{K},\mathbf{p}) = \int_0^T \frac{dt}{T}\langle\psi_B|\mathbf{r}e^{-i\mathbf{K}\cdot\mathbf{r}}|\mathbf{p}+\mathbf{A}(t)\rangle \exp\left\{i(E_B+\omega_\mathbf{K})t - \frac{i}{2}\int^t dt'\left[\mathbf{p}+\mathbf{A}(t')\right]^2\right\}. \quad (5)$$

In the case of the HHG process, the harmonic power (intensity) of the nth harmonic is defined by [16, 19]

$$P_n = \frac{(n\omega)^4}{2\pi c^3}\left|T_n\right|^2, \quad (6)$$

where $T_n = \mathbf{T}_n \cdot \hat{\mathbf{e}}_n^*$ is the T-matrix element for the transition from the initial to the final state and $\hat{\mathbf{e}}_n = \hat{\mathbf{e}}_\mathbf{K}$ the complex unit polarization vector of the nth harmonic photon. Here

$$\mathbf{T}_n = \int_0^T \frac{dt}{T}\mathbf{d}_{fi}(t)e^{in\omega t} \quad (7)$$

is the Fourier component of the time-dependent dipole matrix element $\mathbf{d}_{fi}(t)$. Within the SFA, the time-dependent dipole can be approximated by [19]

$$\mathbf{d}_{fi}(t) \approx \sum_a \mathbf{d}_{fi}^a(t), \quad (8)$$

with the time-dependent dipole moment for the active electron, denoted with the index a,

$$\mathbf{d}_{fi}^a(t) \approx -i\left(\frac{2\pi}{i}\right)^{3/2}\int_0^\infty \frac{d\tau}{\tau^{3/2}}e^{iS_s}\langle\psi_{af}|\mathbf{r}_a|\mathbf{k}_s+\mathbf{A}(t)\rangle\langle\mathbf{k}_s+\mathbf{A}(t-\tau)|\mathbf{r}_a\cdot\mathbf{E}(t-\tau)|\psi_{ai}\rangle, \quad (9)$$

where $\mathbf{k}_s \equiv -\int_{t-\tau}^t dt'\mathbf{A}(t')/\tau$ is the stationary momentum, $S_s \equiv E_f t - \int_{t-\tau}^t dt'[\mathbf{k}_s+\mathbf{A}(t')]^2/2 - E_i(t-\tau)$ the action and $E_i = E_f = -I_\mathrm{P}$, where I_P is the ionization potential.

The ground-state atomic wave function is modeled by a linear combination of Slater-type orbitals obtained using the Hartree-Fock-Roothaan method [25]. For atoms with a p ground state the magnetic quantum number is $m = 0, \pm 1$. Taking into account the fact that for atoms with closed electron shells (Ne, Ar, Kr, Xe) m-changing transitions are forbidden by the Pauli exclusion principle, only three electrons are active. In this case we have [19]

$$\mathbf{d}_{fi}(t) \approx \sum_{a=1,2,3}\mathbf{d}_{fi}^a(t)\big|_{m_i=m_f=m} = \sum_m \mathbf{d}_m(t), \quad (10)$$

where $\mathbf{d}_m(t)$ ($m = 0, \pm 1$) is given by equation (9).

The SFA theory of the (H)ATI process is described in detail in [4]. The observable quantity is the averaged differential ionization rate given by

$$\overline{w}_{\mathbf{p}i}(n) = \frac{N_e}{2l+1}\sum_{m=-l}^{l} w_{\mathbf{p}ilm}(n), \quad (11)$$

where N_e is the number of equivalent electrons in the ionizing shell and $w_{\mathbf{p}ilm}(n) = 2\pi p|T_{\mathbf{p}i}(n)|^2$. Here n is the number of photons absorbed from the laser field such that $n\omega = E_\mathbf{p} + U_\mathrm{P} + I_\mathrm{P}$. The T-matrix element $T_{\mathbf{p}i}(n)$ can be written in the framework of the SFA as the sum

$$T_{\mathbf{p}i}(n) = \int_0^T \frac{dt}{T}e^{i[\mathbf{p}\cdot\boldsymbol{\alpha}(t)+U_1(t)]}\left[\mathcal{T}_{\mathbf{p}i}^{(0)}(t) + \mathcal{T}_{\mathbf{p}i}^{(1)}(t)\right]e^{in\omega t}, \quad (12)$$

where

$$\mathcal{T}_{\mathbf{p}i}^{(0)}(t) = \langle \mathbf{p} + \mathbf{A}(t)|\mathbf{r}\cdot\mathbf{E}(t)|\psi_i\rangle \tag{13}$$

describes the direct ATI process, while

$$\mathcal{T}_{\mathbf{p}i}^{(1)}(t) = -i\int_0^\infty d\tau \left(\frac{2\pi}{i\tau}\right)^{3/2} \langle \mathbf{p}|V|\mathbf{k}_s\rangle\langle \mathbf{k}_s + \mathbf{A}(t-\tau)|\mathbf{r}\cdot\mathbf{E}(t-\tau)|\psi_i\rangle e^{i[S_{\mathbf{k}_s i}(t-\tau)-S_{\mathbf{k}_s i}(t)]} \tag{14}$$

allows for one additional interaction of the liberated electron with its parent ion (HATI process). The phase factor in the previous equation is given by $S_{\mathbf{k}_s i}(t) = \int^t dt'\{[\mathbf{k}_s + \mathbf{A}(t')]^2/2 + I_{\rm P}\} = (\mathbf{k}_s^2/2 + U_{\rm P} + I_{\rm P})t + \mathbf{k}_s\cdot\boldsymbol{\alpha}(t) + U_1(t)$, with $U_1(t) = \int^t \mathbf{A}^2(t')dt'/2 - U_{\rm P}t$ and $\boldsymbol{\alpha}(t) = \int^t \mathbf{A}(t')dt'$.

3. Bicircular field and dynamical symmetries

We use a bichromatic circularly polarized field with coplanar counterrotating components having the angular frequencies $r\omega$ and $s\omega$, which are integer multiples of the same fundamental frequency ω. The corresponding electric-field vector in the xy plane is defined by [7, 8, 9, 26]

$$\mathbf{E}(t) = \frac{i}{2}\left[E_r\hat{\mathbf{e}}_+ e^{-ir\omega t} + E_s\hat{\mathbf{e}}_- e^{-is\omega t}\right] + \text{c.c.}, \tag{15}$$

where $\hat{\mathbf{e}}_\pm = (\hat{\mathbf{e}}_x \pm i\hat{\mathbf{e}}_y)/\sqrt{2}$. In equation (15) E_j and $I_j = E_j^2$ are the amplitude and intensity of the jth field component of helicity h_j ($h_r = 1$, $h_s = -1$). The components of the bicircular field (15) are

$$E_x(t) = \left[E_r\sin(r\omega t) + E_s\sin(s\omega t)\right]/\sqrt{2}, \tag{16}$$

$$E_y(t) = \left[-E_r\cos(r\omega t) + E_s\cos(s\omega t)\right]/\sqrt{2}. \tag{17}$$

Denoting $A_r = E_r/(r\omega)$ and $A_s = E_s/(s\omega)$, for the ponderomotive energy we obtain $U_{\rm P} = (A_r^2 + A_s^2)/4$. The normalized electric-field vector $\mathbf{E}(t)$ and the pertinent normalized vector potential $\mathbf{A}(t)$ for various combinations of $(r,s) \in (1,2),(1,3),(2,3)$ and equal intensities of the field components are presented in figure 1.

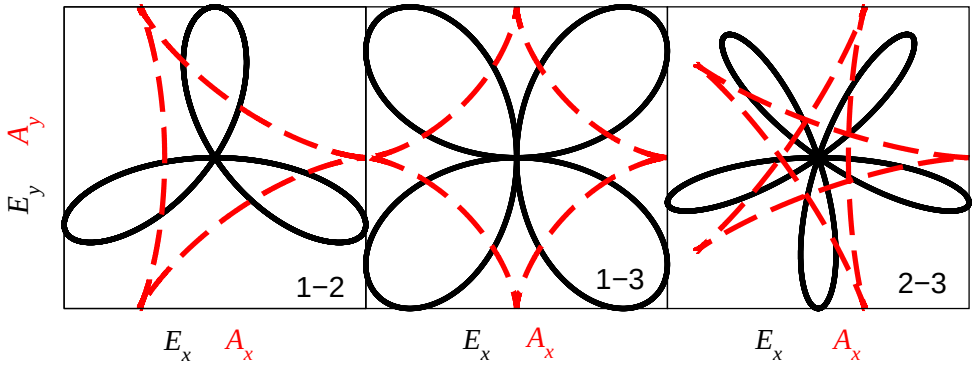

Figure 1. (Color online) Normalized electric-field vector $\mathbf{E}(t)$ (solid black lines) and vector potential $\mathbf{A}(t)$ (dashed red lines) of the $r\omega - s\omega$ bicircular laser field given by equation (15) for equal laser field component intensities and $(r,s) \in (1,2),(1,3),(2,3)$, plotted for $0 \le t \le T$, $T = 2\pi/\omega$.

Since the electric field vector lies in the xy plane, similarly as in references [7, 17], we define the degree of circular polarization $\xi_n = \mathrm{Im}\,(2T_{nx}^* T_{ny})/|T_n|^2$. Then the ellipticity of the emitted harmonic is given by

$$\varepsilon_n = \mathrm{sgn}(\xi_n) \left(\frac{1 - \sqrt{1-\xi_n^2}}{1 + \sqrt{1-\xi_n^2}} \right)^{1/2}. \tag{18}$$

The bicircular field $\mathbf{E}(t)$, as well as the vectors $\mathbf{A}(t)$ and $\boldsymbol{\alpha}(t)$, obey the following dynamical symmetry: the rotation by the angle $\alpha_j = -2\pi j r/(r+s)$ about the z axis is equivalent to the translation in time by $\tau_j = jT/(r+s)$ [16, 19, 27, 28], i.e.

$$R_z(\alpha_j)\mathbf{E}(t) = \mathbf{E}(t+\tau_j), \tag{19}$$

where j is an integer. The diagonal matrix elements of the rotation matrix $R_z(\alpha_j)$ are $\cos\alpha_j$, while the off diagonal elements are $\pm\sin\alpha_j$. We expect that the spectra of HHG and LAR photons as well as the spectra of (H)ATI electrons exhibit the same type of the symmetry [19, 27, 28, 29]. In addition to the discrete rotational symmetry (19), the bicircular fields observe a reflection symmetry about any of the various obvious symmetry axes.

4. Numerical results

In this section, we will present numerical results for the processes HHG, HATI and LAR. As an example, we choose the Ar atom (Ar^+ ion) with a $2p$ ground state for the HHG and HATI (LAR) process whose bound-state energy is -15.75 eV. We use the bicircular field (15) with $r = 1$ and $s = 2$, equal component intensities $I_r = I_s = 1.5 \cdot 10^{14}$ W/cm^2 and the fundamental wavelength 800 nm. For the LAR process the momentum of the incident electron is in the xy plane, such that $\mathbf{p} \cdot \hat{\mathbf{e}}_x = p\cos\theta$.

In figure 2 we present the differential power spectrum coded in false color, as a function of the incident-electron angle (horizontal axis) and the x-ray energy (vertical axis) for the incident-electron energy $E_\mathbf{p} = 50$ eV and the magnetic quantum $m = 1$ number of the ground state (qualitatively similar results are obtained for the $m = -1$ case). The figure is dominated by the superposition of three sine-like wave patterns per cycle, which create conical-like shapes. In [27] these structures are explained by interference of different numbers of classical solutions. Additionally, for the chosen combination $r = 1$ and $s = 2$, the effects of the dynamical symmetry (19) are clearly visible, as explained in section 2. The afore-mentioned reflection symmetry is also obvious, as the pattern is symmetric about any angle that is a multiple of 60°.

In figure 3 we present the harmonic power as a function of the harmonic order for Ar atoms modeled by a realistic $2p$ state with four orbitals [25]. Our numerical results presented in figure 3 confirm the selection rules [5, 7] where the harmonics $n = 3q$ (q integer) are absent, while the harmonics $n = 3q \pm 1$ have the ellipticity $\varepsilon_n = \pm 1$. Additionally, from the left panel of figure 3 it is clearly visible that the intensities of the harmonics $n = 3q - 1$, having the ellipticity $\varepsilon_n = -1$, are different from those of the harmonics $n = 3q + 1$, for which $\varepsilon_n = 1$. Which ones of the harmonics with positive or negative ellipticities are stronger depends on their position in the plateau. The same feature has also been observed in spectra obtained from solutions of the time-dependent Schrödinger equation [18]. The partial spectra for particular values $m = -1$ and $m = +1$ are shown in the right panel of figure 3. The asymmetry between the $\varepsilon_n = -1$ and $\varepsilon_n = 1$ harmonics is also visible for all four possible combinations $(\varepsilon_n, m) = (\pm 1, \pm 1)$ and more pronounced than in the m-averaged case.

The logarithm of the differential ionization rate of Ar atoms is presented as a function of the electron momentum in figure 4. We show the spectra of the so-called direct electrons (electrons that reach the detector without interacting with the parent ion after ionization) as well as those of the rescattered electrons (electrons that undergo exactly one scattering off

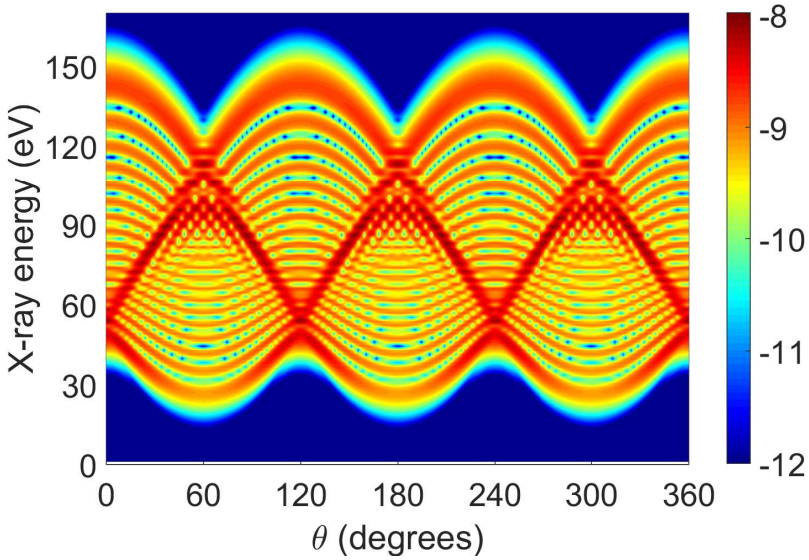

Figure 2. (Color online) Logarithm of the differential power spectrum presented in false color as a function of the incident electron angle and the x-ray energy for laser-assisted radiative recombination of an electron with an Ar^+ ion in the presence of the bicircular laser field (15) with the fundamental wavelength of 800 nm, $I_r = I_s = 1.5 \cdot 10^{14}$ W/cm^2 and $r = 1$, $s = 2$. The incident electron energy is $E_{\mathbf{p}} = 50$ eV and the Ar bound state is $2p$ with the magnetic quantum number $m = 1$.

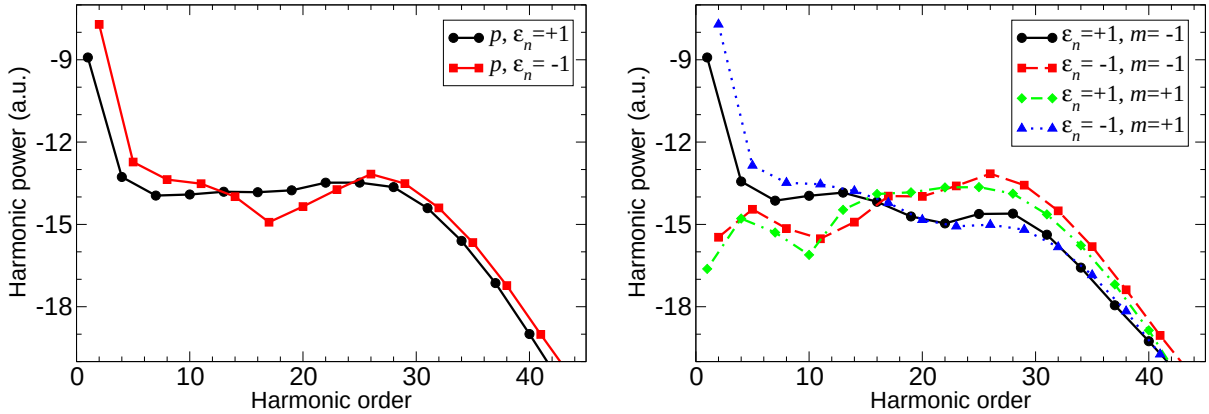

Figure 3. (Color online) Harmonic power as a function of the harmonic order for HHG by the bicircular field (15) for Ar atoms and the field-component wavelengths $\lambda_1 = 800$ nm and $\lambda_2 = 400$ nm ($r = 1$, $s = 2$) and intensities $I_r = I_s = 1.5 \cdot 10^{14}$ W/cm^2. The nth harmonic ellipticity is $\varepsilon_n = \pm 1$ for $n = 3q \pm 1$, where q is an integer. The left panel exhibits the results obtained using the realistic $2p$ ground state, while the right panel displays separate results for specific values of the initial- and final-state magnetic quantum numbers $m_i = m_f = m$.

the parent ion after ionization). As one can see the contribution of the direct electrons to the ionization rate is more then one order of magnitude larger than that of the rescattered electrons. Furthermore, as expected from the streaking condition $\mathbf{p} + \mathbf{A}(t) = \mathbf{0}$ the direct electrons are emitted predominantly in the direction opposite to the vector potential at the time of ionization (i.e. in the directions determined by the emission angles $\theta = 60°, 180°$ and $300°$). The structure

of the rescattered electron spectrum is more complex. It consists of three broad peaks at the emission angles $\theta \approx 60°, 180°$ and $300°$ from which extensions emanate in the clockwise direction, which while becoming weaker and weaker proceed to form concentric rings similar to the ATI rings that are familiar from ionization by linear polarized fields; see, e.g., [30].

It is obvious that both spectra are symmetric with respect to rotations about the z axis by multiples of an angle of 120°. However, in contrast to the spectrum of the rescattered electrons, the direct electron spectrum obeys an additional reflection symmetry about one of the three axes at the angles of $60°, 180°$ and $300°$. The presence or absence of the reflection symmetry allows one to assess whether or not rescattering plays a role in a given spectrum. It should be mentioned that ATI spectra of Ar atoms generated by a bicircular field having an intensity three times lower than the one used in figure 4 have recently been examined in Ref. [31]. The three-fold symmetry as well as traces of rescattered electrons are clearly visible in this experiment.

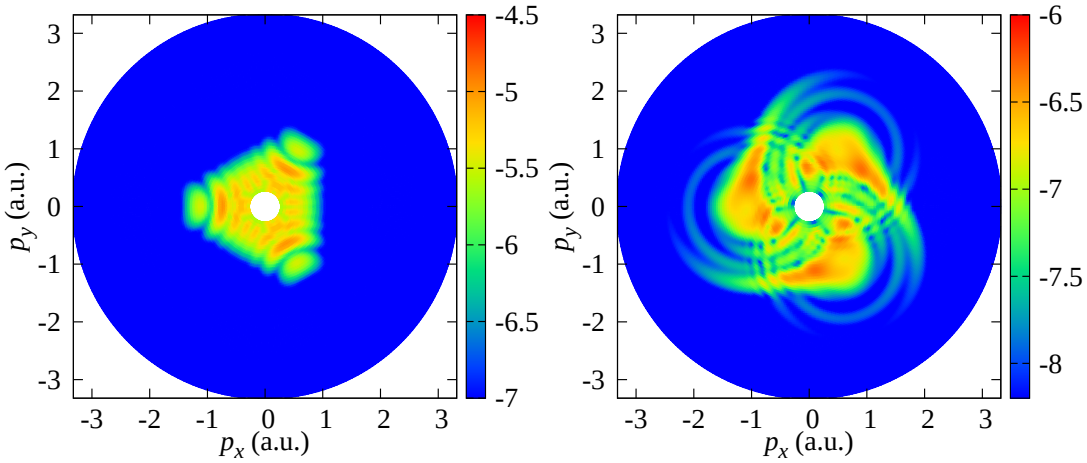

Figure 4. (Color online) Logarithm of the differential ionization rate of Ar atoms presented in the momentum plane for the laser-field parameters as in figure 2. The contribution of the direct (rescattered) electrons is shown in the left (right) panel.

5. Conclusions

We applied the SFA theory to investigate the LAR, HHG and HATI processes in the presence of a bicircular laser field. For the LAR process we numerically calculated the differential power spectrum of the emitted x rays as a function of the incident-electron angle θ for a fixed value of the incoming electron energy $E_{\mathbf{p}}$. The spectrum exhibits symmetry under rotations by an angle of $2\pi/(r+s) = 120°$, which reflects the symmetry of the applied laser field.

Considering the HHG process of argon atoms with a p ground state, we found strong asymmetry in the emission of left- and right-circularly polarized harmonics. According to the selection rules the harmonics $n = 3q \pm 1$, with q an integer, are emitted. The HHG spectra display a strong dependence on the magnetic quantum number m. The asymmetry between emission of circularly polarized harmonics with opposite helicities ($\varepsilon_n = \pm 1$) is important for the investigation of photoelectron circular dichroism in chiral molecules and for x-ray magnetic circular dichroism spectroscopy. These circularly polarized harmonics provide a much-desired table-top source of coherent soft x rays.

We also investigated above-threshold ionization generated by a bicircular field. The photoelectron spectrum presented in the momentum plane is symmetric with respect to rotations by multiples of 120° about the z axis, both for the direct and the rescattered electrons. The direct electron spectrum exhibits an additional symmetry: reflection about one of three different

axes in the xy plane. Since this kind of symmetry is absent for the rescattered electrons, it allows one to assess whether or not rescattering plays a role in a given spectrum.

The combination of attoclock features with the discrete rotational symmetry makes the bicircular field a powerful tool to investigate the electron dynamics on the attosecond time scale. Since a bicircular field develops in a plane, the electron trajectories are two-dimensional and the direct and rescattering ATI structures are well separated. We expect that bicircular fields can be especially useful for the investigation of the dynamics of planar molecules.

We gratefully acknowledge support by the Federal Ministry of Education and Science, Bosnia and Herzegovina.

References

[1] Milošević D B and Ehlotzky F 2003 *Adv. At. Mol. Opt. Phys.* **49** 373
[2] Lein M 2007 *J. Phys. B: At. Mol. Opt. Phys.* **40** R135
[3] Milošević D B and Ehlotzky F 2002 *Phys. Rev.* A **65** 042504
[4] Becker W, Grasbon F, Kopold R, Milošević D B, Paulus G G and Walther H 2002 *Adv. At. Mol. Opt. Phys.* **48** 35
[5] Eichmann H, Egbert A, Nolte S, Momma C, Wellegehausen B, Becker W, Long S and McIver J K 1995 *Phys. Rev.* A **51** R3414(R)
[6] Long S, Becker W and McIver J K 1995 *Phys. Rev.* A **52** 2262
[7] Milošević D B, Becker W and Kopold R 2000 *Phys. Rev.* A **61** 063403
[8] Milošević D B and Sandner W 2000 *Opt. Lett.* **25** 1532
[9] Milošević D B, Becker W, Kopold R and Sandner W 2001 *Laser Phys.* **11** 165
[10] Milošević D B and Becker W 2000 *Phys. Rev.* A **62** 011403(R)
[11] Ceccherini F, Bauer D and Cornolti F 2003 *Phys. Rev.* A **68** 053402
[12] Milošević D B and Becker W 2005 *J. Mod. Opt.* **52** 233
[13] Fleischer A, Kfir O, Diskin T, Sidorenko P and Cohen O 2014 *Nature Photon.* **8** 543
[14] Pisanty E, Sukiasyan S and Ivanov M 2014 *Phys. Rev.* A **90** 043829
[15] Kfir O *et al* 2015 *Nature Photon.* **9** 99
[16] Milošević D B 2015 *Opt. Lett.* **40** 2381
[17] Milošević D B 2015 *J. Phys. B: At. Mol. Opt. Phys.* **48** 171001
[18] Medišauskas L, Wragg J, van der Hart H and Ivanov M Yu 2015 *Phys. Rev. Lett.* **115** 153001
[19] Milošević D B 2015 *Phys. Rev.* A **92** 043827
[20] Fan T *et al* 2015 *Proc. Natl. Acad. Sci. USA* **112** 14206
[21] Yuan K-J and Bandrauk A D 2015 *Phys. Rev.* A **92** 063410
[22] Zuo T and Bandrauk A D 1995 *J. Nonlinear Opt. Phys. Mat.* **4** 533
[23] Bandrauk A D and Lu H Z 2003 *Phys. Rev.* A **68** 043408
[24] Tong X M and Chu S I 1998 *Phys. Rev.* A **58** R2656
[25] Radzig A A and Smirnov B M 1985 *Reference Data on Atoms, Molecules and Ions* (Berlin: Springer)
[26] Milošević D B, Becker W and Kopold R 2001 *Atoms, Molecules and Quantum Dots in Laser Fields: Fundamental Processes* (Conference Proceedings vol 71) ed N Bloembergen, N Rahman and A Rizzo (Bologna: Societá Italiana di Fisica) pp 239–252
[27] Odžak S and Milošević D B 2015 *Phys. Rev.* A **92** 053416
[28] Kramo A, Hasović E, Milošević D B and Becker W 2007 *Laser Phys. Lett.* **4** 279
[29] Hasović E, Kramo A and Milošević D B 2008 *Eur. Phys. J. Spec. Top.* **160** 205
[30] Möller M, Meyer F, Sayler A M, Paulus G G, Kling M F, Schmidt B E, Becker W and Milošević D B 2014 *Phys. Rev.* A **90** 023412
[31] Mancuso C A *et al* 2015 *Phys. Rev.* A **91** 031402(R)